

# Light-Controlled Molecular Shuttles Made from Motor Proteins Carrying Cargo on Engineered Surfaces

Henry Hess,<sup>†</sup> John Clemmens,<sup>†</sup> Dong Qin,<sup>†</sup> Jonathon Howard,<sup>‡</sup> and Viola Vogel<sup>\*†</sup>

*Department of Bioengineering, University of Washington, Seattle Washington 98195, and Max Planck Institute of Molecular Cell Biology and Genetics, 01307 Dresden, Germany*

Received February 21, 2001

## ABSTRACT

Molecular shuttles have been built from motor proteins capable of moving cargo along engineered paths. We illustrate alternative methods of controlling the direction of motion of microtubules on engineered kinesin tracks, how to load cargo covalently to microtubules, and how to exploit UV-induced release of caged ATP combined with enzymatic ATP degradation by hexokinase to turn the shuttles on and off sequentially. These are the first steps in the development of a tool kit to utilize molecular motors for the construction of nanoscale assembly lines.

One of the central challenges in nanotechnology is how to assemble nanoscale building blocks including molecular wires and nanoscale switches into addressable devices, where the building blocks can be either synthesized, self-assembled in solution, or fabricated at the nanoscale. Ideally, a nanoscale conveyor belt would allow us to transport a selected nanoscale item over a defined distance and then facilitate the docking under defined angles with a second item of choice. One labor-intensive approach is to use tips of scanning probe microscopes to pick up, move, and release atoms, single molecules, and nanoscale objects in a controlled manner, one at a time.<sup>1</sup> Nanoscale objects created in this way are therefore pieces of art rather than devices of economical value. Methods need to be developed that allow the parallel assembly of nanoscale building blocks in large numbers. Here we combine methods of micro- and nanofabrication, with molecular assembly, and molecular motors powered chemically by adenosine triphosphate (ATP) to construct molecular shuttles that move under user control. This represents the first step in learning how to construct and operate nanoscale conveyor belts in large numbers.

Key features of conveyor belts are that they (a) are driven by a force-generating motor, (b) transport cargo unidirectionally between well-defined positions, (c) accommodate loading and docking of cargo, and (d) can be externally switched on and off. These features are independent of the

length scale at which conveyor belts are constructed and operated. If operation at the nanoscale is desired, molecular motors are required to generate force to propel cargo. Furthermore, schemes have to be developed to guide molecular movement along precisely controlled tracks, to load and unload cargo, and to control the speed of motion noninvasively. We will review and describe novel approaches that can serve as universal elements of a tool kit to construct and operate molecular shuttles.

**Molecular Motors.** Nature has evolved unique molecules, termed motor proteins, that transport cargo over long distances or rotate loads in an energy-dependent manner. The characteristics of these motor proteins are far superior to all demonstrated miniaturized synthetic engines.<sup>2</sup> Motor proteins generate more force, have better fuel efficiency, and are smaller in size than any man-made device.

Kinesin is a motor protein that transports cargo unidirectionally along cytoskeletal filaments called microtubules,<sup>3,4</sup> which serve as unbranched tracks in cells. In a neuron, for example, kinesin mediates the movement of membrane-bound vesicles from the cell body toward the synapses located at the distal ends of the axon. The tubulin orientation within a microtubule defines the orientation at which kinesin can bind to and move along microtubules. Each kinesin molecule has two “heads”, which bind to microtubules and hydrolyze ATP,<sup>5,6</sup> a 50 nm long semiflexible coiled-coil region, and a “tail”, which is thought to bind to the cargo.<sup>7</sup>

While kinesin was favored recently as a motor for a molecular shuttle due to its small size and processivity, other motor proteins with different characteristics can be utilized

\* Corresponding author. Fax: (206) 685-4434. E-mail: vvogel@u.washington.edu.

<sup>†</sup> University of Washington.

<sup>‡</sup> Department of Physiology and Biophysics, University of Washington, and Max Planck Institute of Molecular Cell Biology and Genetics.

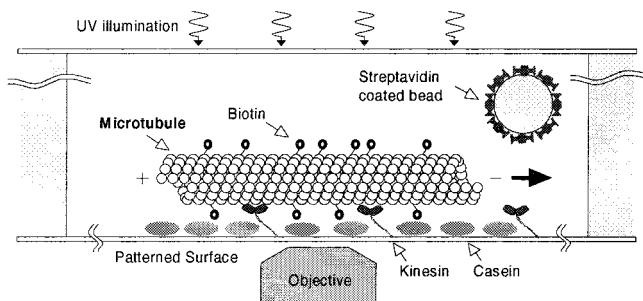


**Figure 1.** Flow cell of the inverted motility. The movement of fluorescently labeled microtubules on a patterned surface covered with the motor protein kinesin is imaged by epifluorescence microscopy. Streptavidin-coated beads representing cargo are mixed into the buffer solution and can bind to biotin linkers conjugated to the microtubules.

for the construction of molecular shuttles. For example, the muscle protein myosin is larger than kinesin and moves along actin filaments, which are more flexible than microtubules.

Reconstituting motor proteins in their active state *ex-vivo* was initially pursued to study the mechanisms by which motor proteins generate force. Such motility assays were established by immobilizing either kinesin (myosin) or microtubules (actin filaments) on glass surfaces, resulting in random motion of single molecules.<sup>8</sup> Later guidance of the motion along lines was achieved.<sup>9,10</sup>

#### Tracks To Guide the Motion of Molecular Shuttles.

Two different approaches are feasible to design molecular shuttles based on kinesin and microtubules: either the microtubules are fixed to the surface and the kinesin is moving similar to cars driving on a highway or (as in our experiments) the kinesin is bound to the surface and the microtubules are propelled by the kinesin analogous to a linear motor.

Utilizing surface-bound microtubules is advantageous for transporting larger, kinesin-coated objects.<sup>11</sup> These can attach to several microtubules at the same time so the cargo does not fall off when the end of a single microtubule is reached. Matching the polarity of the microtubules is achieved through the use of flow fields, which restrict the options to pattern the surface.

“Inverted” motility assays,<sup>12</sup> where the rotationally flexible kinesins are surface bound and propel microtubules as illustrated in Figure 1, are superior for the engineering of tracks with precisely controlled curvature and intersections, since the surface can be arbitrarily patterned.

Guiding in inverted motility assays has previously been achieved by adsorbing the motor proteins in “tracks” on surfaces. The selective adsorption of motor proteins is caused by chemical surface modification (hydrophobic vs hydrophilic regions)<sup>13,14</sup> or preferential adsorption into the nanometer wide grooves of a shear-deposited PTFE film.<sup>10,15</sup> The guiding mechanism is based on Brownian motion: The advancing tip of the microtubule seeks the next kinesin within its reach, while swiveling slightly to the left and right. If the track of kinesins is turning abruptly to one side the tip cannot follow the trail of kinesins and the advancing microtubule detaches from the surface. From the known

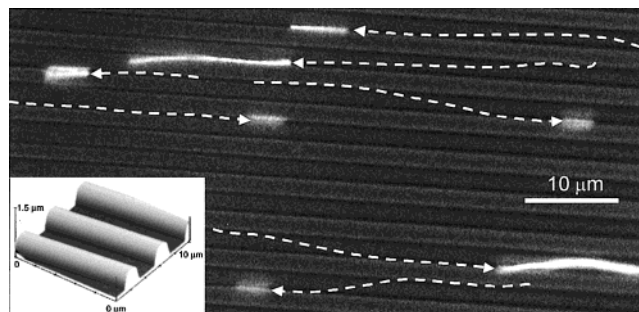


**Figure 2.** Movement of microtubules on a polyurethane surface patterned with 2  $\mu\text{m}$  wide and 1  $\mu\text{m}$  deep channels. The bottom of the channels is in focus; the plateaus in between are out of focus. The inset shows a tapping mode AFM image of the dry polyurethane surface.

stiffness of the microtubule the minimum<sup>16</sup> bending radius that sustains guiding can be estimated to be  $\sim 20 \mu\text{m}$  for a motor density of  $250 \mu\text{m}^{-2}$ .

To achieve sharper turns, larger guiding forces have to be exerted by a different mechanism. Here we introduce micron scale surface topography created by replica molding,<sup>17</sup> providing guiding channels and walls, as a means to direct the motion of microtubules. It can be estimated, that a single kinesin provides enough force (5 pN) to bend a microtubule against a guiding wall in a turn with a bending radius of  $\sim 2 \mu\text{m}$ . With several kinesins pushing the same microtubule, the bending radius would be limited to a minimum of several hundred nanometers.

The motion of microtubules on a kinesin-coated polyurethane surface patterned with 2  $\mu\text{m}$  wide and 1  $\mu\text{m}$  deep channels is clearly constrained by the surface topography, as shown in Figure 2. During the initial adsorption of microtubules from solution, microtubules landing in the direction of the pattern tend to find a groove and stay inside. The most frequent escape mechanism is to bind to a sidewall, slowly climb up and transfer to the next groove. Guiding can also occur on the 2  $\mu\text{m}$  wide plateaus but detachment is more frequently the result. Microtubules landing perpendicular to the pattern move down to the bottom of the groove and up again to the plateau where they subsequently detach.

Using a surface patterned with 50  $\mu\text{m}$  wide grooves, we can study how the microtubule path depends on the angle of approach to a wall (Figure 3). Contrary to the observations by Stracke et al.,<sup>18</sup> who found that microtubules cannot climb walls higher than 286 nm, we see microtubules climbing 1  $\mu\text{m}$  high walls in 80% of the 60 analyzed cases of microtubule–wall encounters if the angle of approach is larger than  $20^\circ$  with respect to the wall. For small angles of approach ( $<20^\circ$ ) between the microtubule and the wall, guiding always occurs and the microtubules follow the wall closely after contact.

None of the above-mentioned guiding methods can prevent “derailing” of a small fraction of microtubules from the intended path. Chemical patterning requires ideal blocking of kinesin adsorption next to the intended tracks, which is challenging on nonideal surfaces. Microscale topographic patterning guides only those microtubules that get trapped

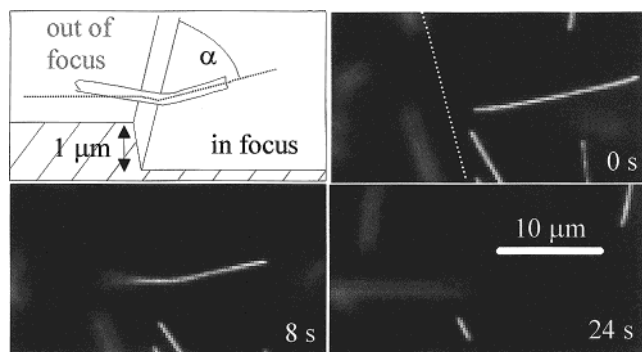


**Figure 3.** Microtubule climbing a wall. The focal plane of the microscope is adjusted to the lower surface. For small angles of approach ( $\alpha < 20^\circ$ ) between the microtubule and the wall, guiding always occurs and the microtubules follow the wall closely after contact. For an intermediate angle of approach ( $20^\circ < \alpha < 65^\circ$ ) guiding as well as climbing occurs. Here, variations of kinesin density and surface topography on the nanoscale may influence the choice of the individual microtubule between guiding and climbing. Large angles of approach ( $\alpha > 65^\circ$ ) always result in a climbing event followed either by detachment of the microtubule or rebinding to the upper surface, as in the case shown here. This microtubule continues its movement deflected by  $13^\circ$  after rebinding to the surface. From this deflection we can determine a wall steepness of  $65^\circ$  assuming the microtubule follows the path of least resistance ( $\cos^2 \sigma = \tan \beta / \tan \alpha$ , with  $\sigma$  the steepness,  $\alpha$  the angle of approach,  $\beta$  the angle after climbing).

in grooves. The optimal solution to the engineering of tracks may thus be a combination of chemical and topographical patterns.

**Loading Cargo.** In the inverted motility assay<sup>19</sup> kinesin is adsorbed to the surface, allowing a microtubule to be linked to cargo through a suitable connector. Since microtubule-bound kinesins move along the microtubule's protofilaments, which are not twisted around the long axis (in contrast to actin), the microtubules are not rotated along their long axis as they are propelled forward by surface-bound kinesins. Cargo hooked up to microtubules thus does not interfere with the gliding motion of the microtubules. The interaction between biotin and streptavidin is widely used in biotechnology to couple proteins to other molecules or surfaces because of the high degree of specificity and strong affinity. An example for the application in motility assays is the binding of biotinylated microtubules to streptavidin-coated surfaces.<sup>20</sup> Here we exploit the well-understood interaction between streptavidin and biotin<sup>21,22</sup> to load microtubules with cargo. Biotinylated tubulin can be polymerized into microtubules through several different methods, resulting in microtubules binding cargo uniformly along its length or restricted to certain regions (see Figure 1).

We used streptavidin-coated superparamagnetic polystyrene beads as cargo for biotinylated microtubules. Mixing an approximately equal number of beads and microtubules into the motility solution and using the solution immediately, we found that microtubules and mostly clumps of beads settle separately to the surface of the flow cell. The Brownian motion of single beads can be observed, whereas clumps of beads tend to be immobile. Moving microtubules randomly pick up beads and transport them across the surface (Figure

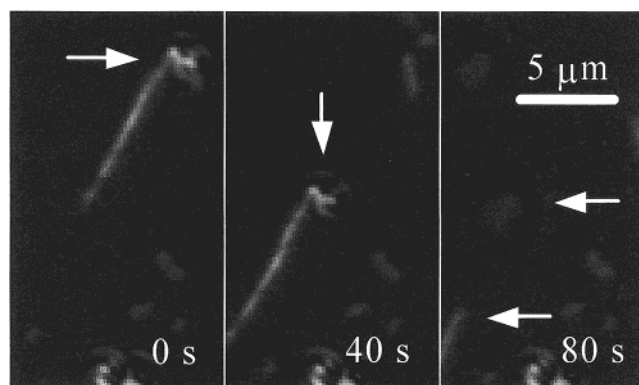


**Figure 4.** A biotinylated microtubule transports a cluster of two streptavidin-coated beads (0 s, 40 s, single arrow) and releases it spontaneously (80 s, one arrow pointing to the beads, one to the microtubule). At the bottom a larger clump of beads is adsorbed to the surface.

4). We observe events where beads are suddenly released from a microtubule, transferred to another microtubule or fused to a larger clump of beads. The speed of the microtubules does not depend on the attachment of cargo, as was expected from the ratio between the viscous drag of a bead (a few femtonewtons) and the force of a kinesin motor (5 pN). Larger clumps of beads (10–100) attached to several microtubules move on complicated paths since the microtubules pull in different directions.

The combination of biotinylated microtubules with streptavidin-coated beads provides us with a mechanism of binding cargo to the microtubules. The tendency of the beads to stick together makes them a model system for studying the assembly of complicated structures, first on a scale easily accessible to optical microscopy and later down to the scale of gold nanoparticles with diameters of 50 nm and smaller. The development of “smart” streptavidin,<sup>23</sup> which binds and unbinds in response to changes of pH or other environmental parameters, or the use of photocleavable biotin can potentially give precise control over loading and unloading.

**Light-Controlled Motility of Molecular Shuttles.** Reversibly *starting* and *stopping* molecular shuttles is challenging because a viable method of controlling motor activity or fuel supply has not yet been developed. Motor activity does not depend critically on conditions like pH or ion concentration.<sup>24</sup> Additionally, ATP consumption of a kinesin-coated surface is very low<sup>25</sup> so that motors can run for many hours on the ATP in the flow cell. The release of certain drugs (e.g., lidocaine) reversibly inhibits kinesin activity,<sup>26</sup> but the removal of these chemicals requires the exchange of the solution in the flow cell.

Caged compounds, which are converted from an inactive “caged” state to an active state after exposure to UV light, provide a nonintrusive method to release a substance. Here we show that using caged ATP<sup>27</sup> in combination with an ATP-consuming enzyme creates a spike in the ATP concentration after exposure to UV light, resulting in micrometer-sized movements of microtubules in a motility assay. The illumination with light can be repeated until the reservoir of



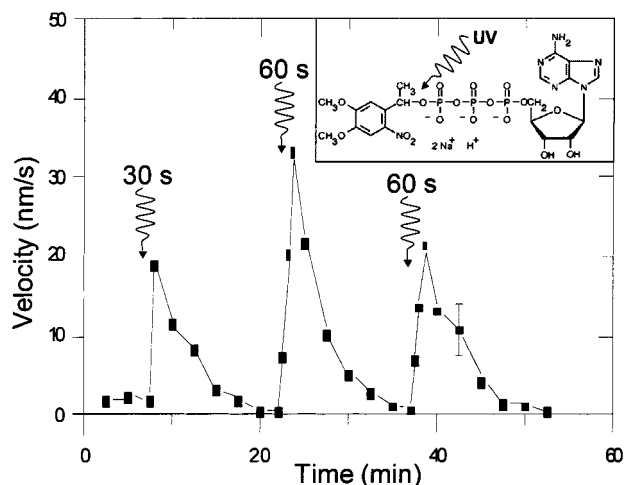


**Figure 5.** Average speed of microtubules ( $N = 10$ ) after exposure of caged ATP to UV light for 30, 60, and 60 s converting 20, 30, and 20% of the initial caged ATP into free ATP. The presence of the ATP-consuming enzyme, hexokinase, leads to a rapid decline of the microtubule velocity. The inset shows the structure of DMNPE-caged ATP.

caged ATP in solution is depleted, so the microtubules move in several discrete steps.

Exposing a flow cell containing a motility solution with 200  $\mu\text{M}$  DMNPE-caged ATP and 50 units/L hexokinase to UV light caused a fast rise of the microtubule speed depending on the light intensity (Figure 5). This was followed by an exponential decrease of the velocity, with a time constant proportional to the concentration of hexokinase, which catalyzes the reaction of glucose and ATP to glucose-6-phosphate and ADP. This process can be repeated until the reservoir of caged ATP is depleted. For experimental convenience the illumination time was chosen to be 30 s (release of 20% of caged ATP), while the hexokinase concentration was chosen to stop the microtubules in about 10 min. The maximum velocity was less than 5% of the velocity at saturating ATP concentrations (800 nm/s). Each light pulse caused the microtubules to move a distance of 4–6  $\mu\text{m}$ , whereas in the absence of hexokinase the microtubules stop after approximately 50  $\mu\text{m}$  within 3 h.

DMNPE-caged ATP acts as a competitive inhibitor for kinesin. By measuring the microtubule speed at an ATP concentration of 10  $\mu\text{M}$  for varying concentrations of caged ATP, we determined an enzyme:inhibitor dissociation constant  $K_i$  of  $175 \pm 70 \mu\text{M}$  (standard error), in agreement with the value of 120  $\mu\text{M}$  quoted by Higuchi et al.<sup>28</sup> The inhibition of kinesin activity by caged ATP and the accumulated products ADP and phosphate limit the initial concentration of caged ATP to roughly 0.5 mM. Above this concentration the increase of the supply of caged ATP is offset by the need to release more ATP in order to maintain the speed. Since the concentration of motors is in the nanomolar range, the reservoir of caged ATP can last for  $\sim 10^5$  steps per motor in the absence of hexokinase, corresponding to a traveled distance of 800  $\mu\text{m}$ . Adding hexokinase increases ATP consumption by a factor of 10–100. The application of caged ATP to fuel molecular shuttles is clearly in the transport of cargo across short distances, preferentially less than 10  $\mu\text{m}$ .

The molecular system constructed to move the shuttles for a defined distance has many interacting elements. Concentrations of ATP, caged ATP, ADP, hexokinase, the activity of kinesin and hexokinase, the quantum yield of the uncaging reaction, the temperature, light intensities, and the mutual dependencies between these parameters have to be measured in order to predict the distance moved as a function of the illumination time. Consequently, using a single, long illumination of controlled duration to move the shuttles a given distance is connected with large uncertainties. It will be more reliable to break the movement into several smaller steps, monitor the progress, and adjust the number of light pulses. Ultimately, the wide range of step sizes, from micrometers possibly down to an elementary step of 8 nm,<sup>7</sup> spans from the dimensions of MEMS devices down to the size of single proteins.

The concept of a *molecular shuttle* relies on solutions to the key issues of nanoscale transport: guidance, loading, and discrete movement. This paper presents a set of three tools to solve these problems based on the kinesin–microtubule system. Guiding the motion by a topographical pattern, loading through linking streptavidin-coated cargo to biotinylated microtubules, and moving for defined distances by simply controlling the exposure to UV light are principles, which in combination can be used to build a functional molecular shuttle.

#### Materials and Methods. Motility Assays and Microscopy.

The motility assays (Figure 1) were performed in 60  $\mu\text{m}$  high and 1 cm wide flow cells built according to ref 12 at a temperature of 20  $^\circ\text{C}$ . First, casein (0.5 mg/mL, Sigma) dissolved in BRB80 (80 mM PIPES, 1 mM  $\text{MgCl}_2$ , 1 mM EGTA, pH 6.9) was adsorbed for 5 min to reduce denaturation of kinesin. Then the kinesin solution (total protein concentration 8  $\mu\text{g/mL}$ , 6 nM active motors as determined by a radioactively labeled ATP assay, BRB80 buffer) was adsorbed for 5 min and exchanged against different motility solutions described below. Flow cells were either sealed with oil or kept hydrated in a moist environment. A Leica DMIRBE optical microscope with a 100 $\times$  oil objective (N.A.1.30), a Hamamatsu ORCAII camera, and Openlab software (Improvision) were used to image rhodamine-labeled microtubules by epifluorescence microscopy, beads by differential interference contrast microscopy, and patterned surfaces by bright field microscopy.

**Kinesin and Microtubules.** A kinesin construct consisting of the wild-type, full-length *Drosophila melanogaster* kinesin heavy chain and a C-terminal His tag was expressed in *Escherichia coli* and purified using a Ni-NTA column. The eluent contained functional motors with a density of 100 nM and was used as stock solution after adding 10% sucrose. Tubulin was purified from bovine brain, fluorescently labeled with rhodamine and polymerized into microtubules according to ref 16. The microtubules with a length between 2 and 20  $\mu\text{m}$  were 100-fold diluted and stabilized in 10  $\mu\text{M}$  Taxol (Sigma).

**Patterned Surfaces.** Patterned films of polyurethane (Norland Products, NOA73) with feature size ranging from 2 to

10  $\mu\text{m}$  were prepared on no. 1.5 coverslips by replica molding.<sup>17</sup> The thin (20  $\mu\text{m}$ ) and transparent polymer films made in situ imaging of the microtubules possible. AFM images (tapping mode, Digital Instruments Nanoscope III) of the dry pattern show a wall steepness of at least 70° and a RMS roughness of 1.2 nm measured on a 500 nm  $\times$  500 nm area. For the bead and caged-ATP assays, coverslips were coated with shear-deposited PTFE films. These films can guide motion in the direction of shear, but we did not optimize the motor density to take advantage of this effect.<sup>15</sup> The motility solution for polyurethane (PU) assays consisted of 1000-fold diluted rhodamine-labeled microtubules, 1 mM ATP, 0.2 mg/mL casein, 10  $\mu\text{M}$  Taxol, and an oxygen-scavenging system to reduce photobleaching<sup>30</sup> (20 mM glucose, 0.02 mg/mL glucose oxidase, 0.008 mg/mL catalase, 0.5% BME).

**Biotin-Streptavidin.** Biotinylated microtubules<sup>20</sup> were prepared by polymerizing 5  $\mu\text{L}$  of biotinylated tubulin (biotin-XX from Molecular Probes) in 4 mM  $\text{MgCl}_2$ , 1 mM GTP, 5% DMSO, and BRB80 buffer for 15 min at 37 °C, then adding 10  $\mu\text{L}$  of rhodamine-labeled tubulin, and polymerizing for another 30 min. The microtubules were then stabilized in BRB80 plus 10  $\mu\text{M}$  Taxol (Wyseth Amherst). This protocol resulted in microtubules with a strongly biotinylated, nonfluorescent seed and less biotinylated, fluorescent ends. Superparamagnetic streptavidin beads (Pierce No. 21344) with a diameter between 0.5 and 1.5  $\mu\text{m}$  were washed three times in BRB80 and vortexed vigorously. The bead motility solution consisted of 1000-fold diluted microtubules, 100-fold diluted beads, 1 mM ATP, 0.2 mg/mL casein, 10  $\mu\text{M}$  Taxol, and the oxygen-scavenging system. The number of microtubules and beads was roughly equal.

**Caged ATP.** 1-(4,5-Dimethoxy-2-nitrophenyl)ethyl caged ATP (Molecular Probes), photocleavable with 365 nm UV light, was dissolved in BRB80. Exposure to UV light from the mercury arc lamp of the microscope using a DAPI filter set led to complete release of ATP in a few seconds. Light from a UV lamp (UVP, UVL-28) mounted on the microscope released 20% of the caged ATP within 30 s, providing a convenient time scale to control the ATP concentration. Hexokinase (Sigma H-5625) with a concentration of 25, 50, and 100 units/L, was used to reduce the ATP concentration by 50% in 6, 3, and 1 min in the presence of 20 mM glucose. The motility solution consisted of 1000-fold diluted microtubules, 50  $\mu\text{M}$  ATP, 200  $\mu\text{M}$  DMNPE-caged ATP, 50 units/L hexokinase, 0.2 mg/mL casein, 10  $\mu\text{M}$  Taxol, and the oxygen-scavenging system (including the 20 mM glucose).

**Acknowledgment.** We thank Rutilio Clark for the preparation of kinesin. The Project was funded by NASA grant NAG5-8784, J.C. thanks the Center for Nanotechnology at the University of Washington for support through an IGERT scholarship. H.H. was supported by the Alexander-von-Humboldt foundation.

## References

- (1) Eigler, D. M.; Schweizer, E. K. *Nature* **1990**, *344*, 524–6.
- (2) Jager, E. W.; Smela, E.; Inganas, O. *Science* **2000**, *290*, 1540–5.
- (3) Brady, S. T. *Nature* **1985**, *317*, 73–75.
- (4) Vale, R. D.; Reese, T. S.; Sheetz, M. P. *Cell* **1985**, *42*, 39–50.
- (5) Yang, J. T.; Saxton, W. M.; Stewart, R. J.; Raff, E. C.; Goldstein, L. S. B. *Science* **1990**, *249*, 42–47.
- (6) Stewart, R. J.; Thaler, J. P.; Goldstein, L. S. B. *Proc. Natl. Acad. Sci. U.S.A.* **1993**, *90*, 5209–5213.
- (7) Coy, D. L.; Wagenbach, M.; Howard, J. *J. Biol. Chem.* **1999**, *274*, 3667–71.
- (8) Harada, Y.; Yanagida, T. *Cell Motil Cytoskeleton* **1988**, *10*, 71–6.
- (9) Turner, D. C.; Chang, C.; Fang, K.; Brandow, S. L.; Murphy, D. B. *Biophys. J.* **1995**, *69*, 2782–2789.
- (10) Suzuki, H.; Oiwa, K.; Yamada, A.; Sakakibara, H.; Nakayama, H.; Mashiko, S. *Jpn. J. Appl. Phys. Part 1* **1995**, *34*, 3937–3941.
- (11) Limberis, L.; Stewart, R. J. *Nanotechnology* **2000**, *11*, 47–51.
- (12) Howard, J.; Hunt, A. J.; Baek, S. *Methods Cell Biol.* **1993**, *39*, 137–47.
- (13) Suzuki, H.; Yamada, A.; Oiwa, K.; Nakayama, H.; Mashiko, S. *Biophys. J.* **1997**, *72*, 1997–2001.
- (14) Nicolau, D. V.; Suzuki, H.; Mashiko, S.; Taguchi, T.; Yoshikawa, S. *Biophys. J.* **1999**, *77*, 1126–34.
- (15) Dennis, J. R.; Howard, J.; Vogel, V. *Nanotechnology* **1999**, *10*, 232–236.
- (16) Gittes, F.; Mickey, B.; Nettleton, J.; Howard, J. *J. Cell Biol.* **1993**, *120*, 923–934.
- (17) Xia, Y. N.; Rogers, J. A.; Paul, K. E.; Whitesides, G. M. *Chem. Rev.* **1999**, *99*, 1823–1848.
- (18) Stracke, P.; Bohm, K. J.; Burgold, J.; Schacht, H. J.; Unger, E. *Nanotechnology* **2000**, *11*, 52–6.
- (19) Howard, J.; Hunt, A. J.; Baek, S. *Methods Cell Biol.* **1993**, *39*, 137–147.
- (20) Gittes, F.; Meyhofer, E.; Baek, S.; Howard, J. *Biophys. J.* **1996**, *70*, 418–29.
- (21) Wong, J.; Chilkoti, A.; Moy, V. T. *Biomol. Eng.* **1999**, *16*, 45–55.
- (22) Grubmuller, H.; Heymann, B.; Tavan, P. *Science* **1996**, *271*, 997–9.
- (23) Stayton, P. S.; Nelson, K. E.; McDevitt, T. C.; Bulmus, V.; Shimoboji, T.; Ding, Z.; Hoffman, A. S. *Biomol. Eng.* **1999**, *16*, 93–9.
- (24) Bohm, K. J.; Stracke, R.; Unger, E. *Cell Biol. Int.* **2000**, *24*, 335–41.
- (25) Howard, J.; Hudspeth, A. J.; Vale, R. D. *Nature* **1989**, *342*, 154–158.
- (26) Miyamoto, Y.; Muto, E.; Mashimo, T.; Iwane, A. H.; Yoshiya, I.; Yanagida, T. *Biophys. J.* **2000**, *78*, 940–9.
- (27) Dantzig, J. A.; Higuchi, H.; Goldman, Y. E. *Methods Enzymol.* **1998**, *291*, 307–48.
- (28) Higuchi, H.; Muto, E.; Inoue, Y.; Yanagida, T. *Proc. Natl. Acad. Sci. U.S.A.* **1997**, *94*, 4395–400.
- (29) Wittmann, J. C.; Smith, P. *Nature* **1991**, *352*, 414–417.
- (30) Kishino, A.; Yanagida, T. *Nature* **1988**, *334*, 74–6.

NL015521E